Fish and Shellfish Immunology 92 (2019) 629–636

Contents lists available at ScienceDirect

Fish and Shellfish Immunology

journal homepage: www.elsevier.com/locate/fsi

Full length article

Intestinal bacterial signatures of the "cotton shrimp-like" disease explain the change of growth performance and immune responses in Pacific white shrimp (*Litopenaeus vannamei*)

Li Zhou[a,b], Chengzhuang Chen[b], Jia Xie[b], Chang Xu[b], Qun Zhao[b], Jian G. Qin[c], Liqiao Chen[d], Erchao Li[a,b,*]

[a] Key Laboratory of Tropical Biological Resources of Ministry of Education, Hainan University, Haikou, Hainan, 570228, China
[b] Department of Aquaculture, College of Marine Sciences, Hainan University, Haikou, 570228, Hainan, China
[c] School of Biological Sciences, Flinders University, Adelaide, SA, 5001, Australia
[d] School of Life Sciences, East China Normal University, Shanghai, 200241, China

ARTICLE INFO

Keywords:
Intestinal microbiota
"Cotton shrimp-like" disease
Growth performance
Immune responses
Litopenaeus vannamei

ABSTRACT

Imbalance of intestinal microbiota has been recognized in aquatic animals infected with various diseases. However, the signature of intestinal bacteria of the "cotton shrimp-like" disease in the Pacific white shrimp *Litopenaeus vannamei* remains unknown. This study investigates the composition, diversity, microbial-mediated function and interspecies interaction of intestinal microbiota on shrimp with different health status using 16S rRNA gene high-throughput sequencing. Meanwhile, the growth performance and the mRNA expression of innate immune gene in hepatopancreas were also investigated. The growth performance and the mRNA expression of innate immune genes (e.g., crustin, toll, and immune deficiency genes) in the hepatopancreas were significantly decreased in diseased shrimp compared with healthy shrimp. Bacteria of the family *Rickettsiaceae* and genus *Tenacibaculum* were exclusively enriched and significantly increased in diseased shrimp, respectively, whereas, the *Actinobacteria* class dramatically deceased. The diseased shrimp exhibited higher ACE and Chao1 indices and lower complexity of intestinal interspecies interaction than healthy shrimp. Microbial-mediated functions predicted by PICRUSt showed that 83% KEGG pathway including nutrient absorption and digestion significantly increased in diseased shrimp. This study provides an overview on the interplay among the "cotton shrimp-like" disease, intestinal microbiota, growth performance and host immune responses from an ecological perspective.

1. Introduction

It has been widely recognized that intestine microbiota can promote host health by acting as a barrier against pathogen invasion and stimulating the host immune response [1,2]. As a result, the intestinal microbiota dysbiosis in composition, diversity, and microbial-mediated function is usually associated with host disease [3,4]. However, the causality of intestinal microbial dysbiosis in diseased shrimp is unclear. The changes in intestinal microbiota may provide an indication of signature characteristics in diseased shrimp. The intestinal microbial signatures of shrimp diseases including white feces syndrome [5], white spot syndrome [6], hepatopancreatic necrosis disease [7] have been studied. However, in all these diseases, the pattern of microbiota changes is inconsistent. For instance, a reduction of bacterial community diversity was observed in some diseased shrimp [3,5], but the diversity of intestinal microbial community in other diseased shrimp is higher than that in healthy ones [8]. As the intestinal microbiota plays an important role in host health, research on the dysbiosis of microbiota is gaining popularity to understand the relationships of host health, immunity and disease resistance [9]. At present, however, the research on the correlation between dysbiosis of intestinal microbiota and shrimp disease epidemics is still in its infancy.

The "cotton shrimp-like" disease is an emerging shrimp disease in the aquaculture of Pacific white shrimp. The obvious clinical signs of "cotton shrimp-like" disease is soft shell, inactivity, slight white opaque appearance of muscle, empty digestive tract, and hepatopancreas atrophy. It does not cause mass mortality, but can seriously reduce shrimp body size, thus lead to yield losses and unmarketable shrimp.

* Corresponding author. Key Laboratory of Tropical Biological Resources of Ministry of Education, Hainan University, Haikou, Hainan, 570228, China.
E-mail address: ecli@bio.ecnu.edu.cn (E. Li).

https://doi.org/10.1016/j.fsi.2019.06.054
Received 11 May 2019; Received in revised form 24 June 2019; Accepted 28 June 2019
Available online 29 June 2019
1050-4648/

While, the “cotton shrimp” disease has generally been recognized by the white opaque appearance of muscle is primarily linked to microsporidian infections [10]. It resulted in mass mortality of shrimp farming [11]. Because the clinical sign of “cotton shrimp-like” disease is similar to the “cotton shrimp” disease, local shrimp farmers also call the “cotton shrimp-like” disease as “cotton shrimp” disease. However, those two diseases are different. Unfortunately, to date, the pathogen of “cotton shrimp-like” disease is unknown and the information about pathological characteristics, immune response is not available.

In this study, 16S rRNA gene high-throughput sequencing was used to characterize intestinal bacterial signatures of “cotton shrimp-like” disease. The interplay among “cotton shrimp-like” disease infection, intestinal bacterial, growth performance, and immune response were fully discussed. The results provide an initial step towards preventing and controlling the epidemic of this disease.

2. Materials and methods

2.1. Shrimp collection

Shrimps were collected from a farm in Wenchang, Hainan, China. The *L. vannamei* larvae of the same origin were introduced into the pond on October 8, 2017 with a stocking density of 180,000 individuals per pond. The size and depth of the pond are approximately 667 m^2 and 1.5 m, respectively. Shrimp were fed four times per day and the pond received seawater of 28‰ salinity with a 5% daily water exchange rate. Diseased shrimp emerged in the 5th pond after 40 days cultivation. The diseased shrimp showed obvious clinical signs, such as soft shell, inactivity, slight white opaque appearance of muscle, empty digestive tract, and atrophic hepatopancreas. According to the clinical signs, the shrimp were categorized into healthy and diseased group. We collected sample in the 5th pond after 43 days of first occurrence of the disease. During these days, diseased shrimp displayed obvious clinical signs as we described previously. The surface of each shrimp was sterilized with 70% ethanol, and the intestine and hepatopancreas were aseptically extracted and placed into a 1.5 ml sterile centrifuge tube, respectively. Considering the inter-individual variation of intestinal microbiota, six shrimps were pooled as one sample, with five samples in total per group. Sample was collected and immediately stored in liquid nitrogen before being transferred to the lab for preservation at −80 °C.

2.2. DNA extraction and sequencing

Total bacterial DNA from intestine was extracted using the E.Z.N.A.® stool DNA Kit (Omega, USA) according to the manufacturer's instruction. The quality and concentration of the extracted DNA were measured using a NanoDrop 2000 spectrophotometer (Thermo Fisher Scientific). The V3–V4 region of the bacteria 16S ribosomal RNA gene was amplified by PCR using primers 338F (5′ ACTCCTACGGGAGGCA GCA 3′) and 806R (5′ GGACTACHVGGGTWTCTAAT 3′). Unique barcodes were added to each primer to distinguish different PCR products. PCR was performed in the 25 μL reaction system containing 5 μL of 5 × reaction buffer, 5 μL of 5 × GC buffer, 2 μL of dNTP (2.50 mM), 1 μL of forward primer (10 μM), 1 μL of reverse primer (10 μM), 2 μL of DNA template, 8.75 μL of ddH_2O, 0.25 μL of Q5® high-fidelity DNA polymerase (NEB). The PCR conditions were as follows: initial denaturation at 98 °C for 2 min, followed by 26 cycles of denaturation at 98 °C for 15 s, annealing at 55 °C for 30 s; extension at 72 °C for 30 s, and final extension at 72 °C for 5 min. Purified PCR products were subjected to Illumina MiSeq PE300 platform (Shanghai Personal Biotechnology Co., Ltd, China), generating paired-end reads. The sequences obtained in this paper are available in SRA with the accession number SRP192810.

2.3. Growth performance evaluation

Thirty diseased and thirty healthy shrimps were collected to detect growth performance. Growth performance parameters including body length, body weight, condition factor, and hepatosomatic index were determined individually, and the condition factor and hepatosomatic index were calculated as follows:

Condition factor (%) = body weight (g)/(body length, $cm)^3 \times 100\%$

Hepatosomatic index (%) = hepatosomatic weight (g)/body weight (g) × 100%

2.4. Quantitative real-time PCR

Hepatopancreas is an important immune organ in shrimp and plays a key role by synthesizing immune factors [12]. The expression of several important innate immunity genes including penaeidin-3a, crustin, anti-lipopolysaccharide factor (ALF), prophenoloxidase (ProPO), toll and immune deficiency (IMD) gene in the hepatopancreas were determined by quantitative real time PCR (qPCR). Total RNA was extracted from hepatopancreas by using RNA isolater total RNA extraction reagent (Vazyme, China). The NanoDrop 2000 spectrophotometer (Thermo Scientific) was used to measure the amount of RNA. Visualization of the 28S/18S ribosomal RNA ratio on a 1% agarose gel was used to assess the RNA quality for each sample. Total RNA (1 μg) was used to synthesize the complementary DNA by a Hi-Script II Q RT SuperMix for qPCR (+gDNA wiper) (Vazyme, China) according to the manufacturer's instruction. Real-time PCR was conducted in the QuantStudio™ 6 Flex Real-Time PCR system (Thermo Fisher Scientific). EF-1α was chosen as the internal control to normalize the data. The primers for the genes penaeidin-3a [13], crustin [14], AIF [15], ProPO [16], IMD,Toll [17], EF-1α [18] were obtained from previous studies. The mixture for qPCR contained 10 μL of 2 × ChamQ Universal SYBR qPCR Master Mix (Vazyme, China), 2 μL of cDNA, 1 μL of forward and reverse primers (5 μM), and 7 μL nuclease-free water. The program for the qPCR reaction was 95 °C for 30 s, 40 cycles at 95 °C for 10 s and 60 °C for 30 s. The melting curves for the amplified products were generated to ensure the specificity of assays at the end of each PCR. Gene expression quantification was calculated using the 2-ΔCT method. All assays were performed in triplicate.

2.5. Bioinformatics and statistical analysis

The raw paired-end readings were then subjected to a quality-control procedure using QIIME (versionv1.8.0) [19]. Operational taxonomic units (OTUs) were defined as sequences clustered with a threshold of 97% similarity using UCLUST [20]. The most abundant sequence in the OTU was selected as the representative sequence and then taxonomically assigned in the Greengenes database (release 13.8) [21]. Alpha diversity indices (Ace, Chao 1, Simpson, and Shannon) were calculated by QIIME. T-test was used to identify the differentially abundant phyla *Chlorobi* and *Plactomycetes*, then spearman's correlation analyses were employed to test the correlations between phyla *Chlorobi*, *Plactomycetes* and richness index. Non-metric multidimensional scaling (NMDS) and analysis of similarity (ANOSIM) were performed to evaluate the overall differences in bacterial community structure based on Bray-Curtis distance metrics in PAST [22]. Venn diagram was constructed to identify the shared and unique OTUs. Linear discriminant analysis (LDA) effect size (LEfSe) was applied to identify statistically significant taxa (biomarkers) between healthy and diseased shrimp [23]. The PICRUSt was used to predict the functional profiling of the intestinal microbiota with high cost performance that uses evolutionary modeling to predict metagenomes from 16S data and a reference genome database [24]. Predicted functional pathways were annotated by using the Kyoto Encyclopedia of Genes and Genomes (KEGG) at levels 1, 2 and 3. Intestinal microbiota interspecies interaction between

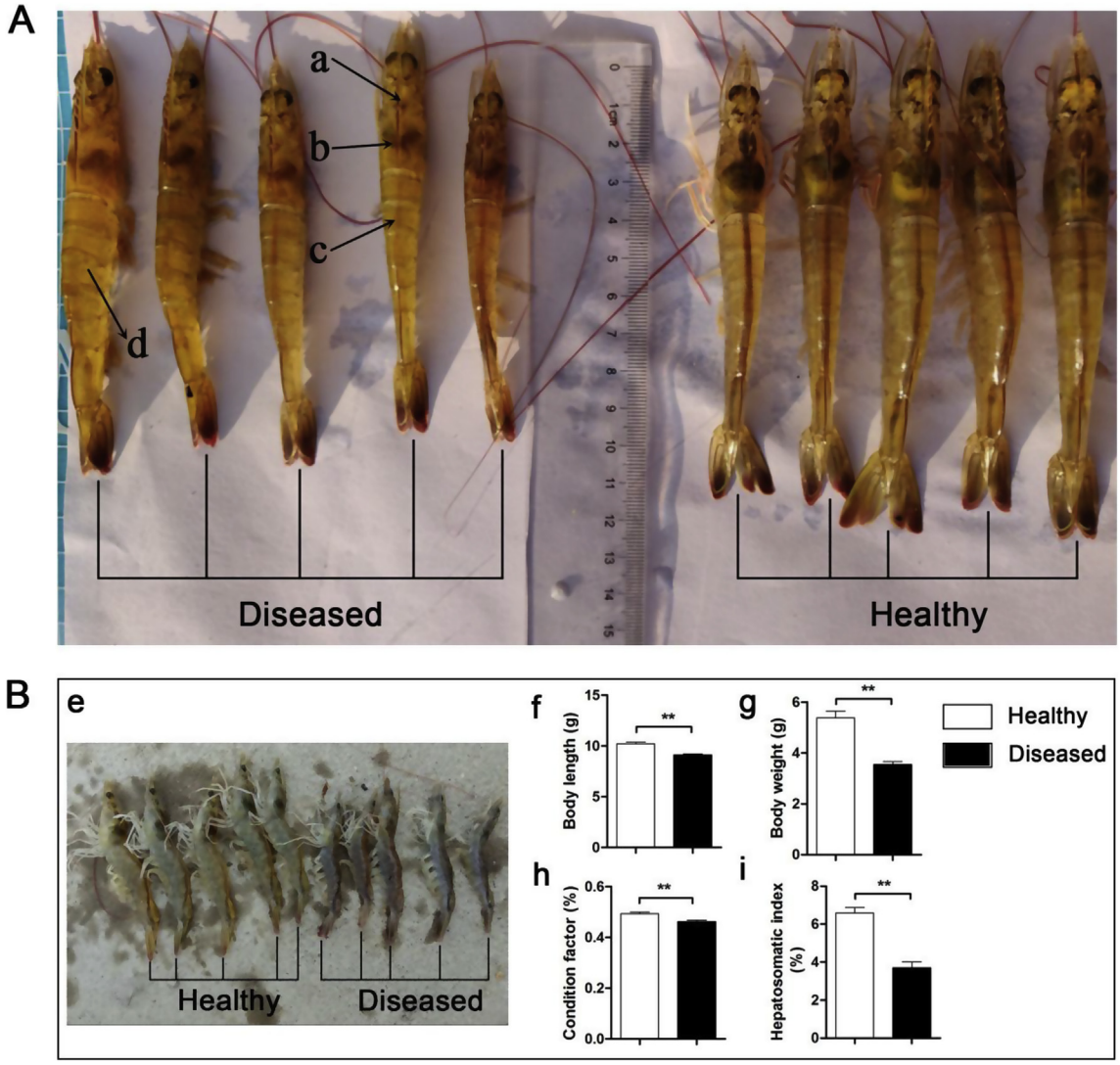

Fig. 1. Typical clinical signs of "cotton shrimp-like" disease (A) and growth performance of shrimp (B). (a) empty stomach; (b) hepatopancreas atrophy; (c) empty intestine; (d) soft shells; (e) diseased shrimp exhibited smaller size then healthy shrimp; (f) body length; (g) body weight; (h) condition factor; (i) Hepatosomatic index. All values are means ± SEM (n = 30), An asterisk (**) indicates a significant difference ($P < 0.01$).

dominant class with abundances in the top 50 were calculated by using Mothur. Constructing interspecies interaction network for the dominant class with Rho > 0.6 and $P < 0.01$. The network properties were calculated and visualized in Gephi [25]. The data are all presented as means ± standard error (SE). Statistical analysis was performed using SPSS software 15.0 (IBM, USA), and the *t*-test was used to analyze differences between groups. Significance was set at $P < 0.05$.

3. Results

3.1. Typical clinical signs of "cotton shrimp-like" disease and growth performance

The diseased shrimp exhibited obvious clinical signs of the "cotton shrimp-like" disease (Fig. 1A), such as a soft shell, inactivity, slight white opaque appearance of muscle, empty digestive tract, and atrophic hepatopancreas. The average weight and length of healthy shrimp were 5.38 ± 0.26 g and 10.23 ± 0.15 cm, respectively. While the average weight and length of diseased shrimp were 3.55 ± 0.12 g and 9.12 ± 0.11 cm, respectively. Growth performance included body length, body weight, condition factor, and hepatosomatic index in diseased shrimp were significantly lower than those in healthy shrimp (Fig. 1B).

3.2. Innate immune response

Comparing with healthy shrimp, the expression of crustin, IMD, and Toll were significantly lower in the diseased shrimp than in the healthy shrimp (Fig. 2B, E, F). indicating that disease markedly reduces the shrimp immune response. The expression of penaeidin-3a, ALF, and ProPO were lower in the diseased shrimp than in the healthy shrimp, but no significant difference was detected (Fig. 2A, C, D).

3.3. Differences in bacterial community composition, diversity and structure

A total of 359,775 high-quality sequences were obtained from ten samples with an average of 35,978 sequences per sample. The dominant phyla in all sample were *Proteobacteria* (49.3%) followed by *Tenericutes* (26.5%) and *Bacteroidetes* (13.5%) (Fig. 3A), their abundance accounting for 89.3% of the total reads. At the family level, *Rickettsiaceae* was specifically enriched in the intestine of diseased shrimp (Fig. 3D), while in the intestine of healthy shrimp, it was no detected. LEfSe analysis revealed eight and six biomarkers with significantly higher relative abundance in healthy and diseased shrimp, respectively

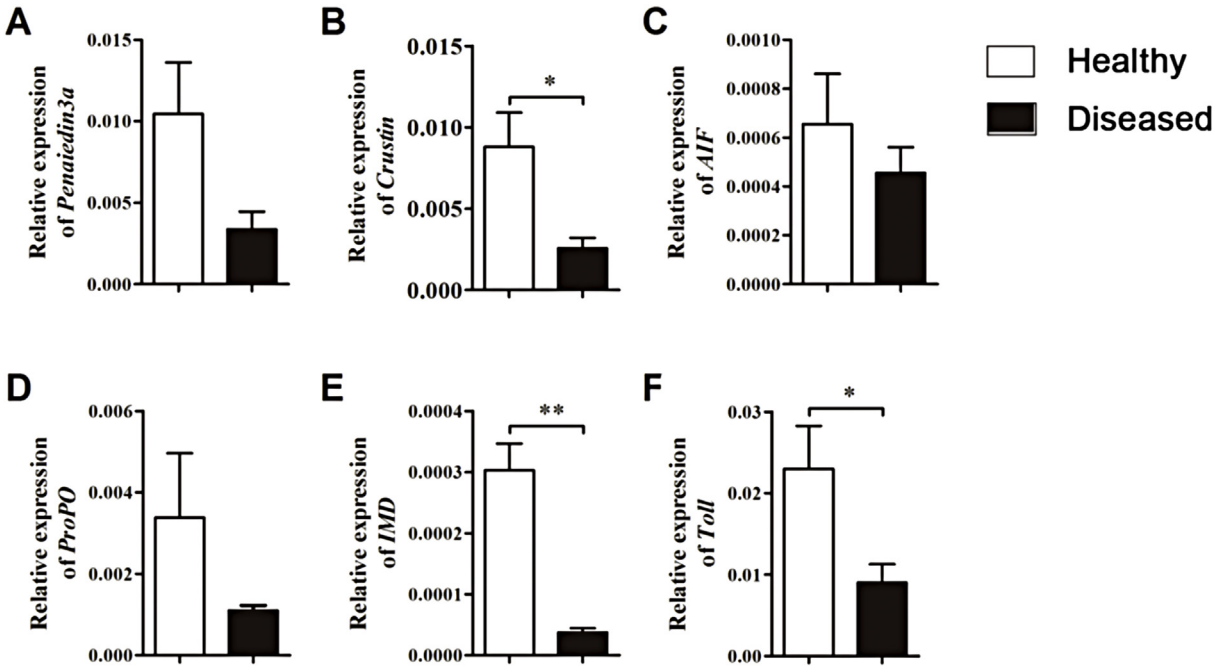

Fig. 2. Relative mRNA expression levels of innate immune gene in hepatopancreas. (A) penaeidin-3a mRNA expression. (B) crustin mRNA expression. (C) Anti lipopolysaccharide factor (ALF) mRNA expression. (D) prophenoloxidase (proPO) mRNA expression. (E) Immune deficiency (IMD) mRNA expression. (F) Toll mRNA expression. $^{*}P < 0.05$, $^{**}P < 0.01$.

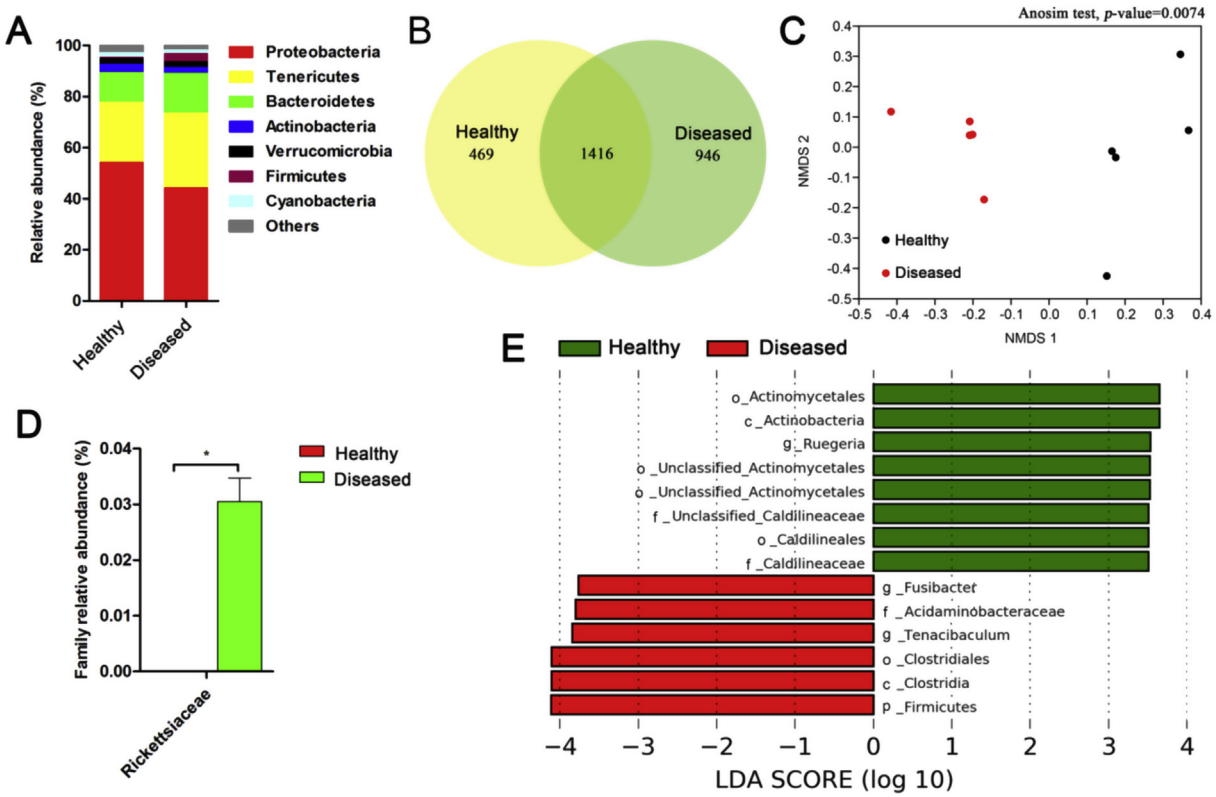

Fig. 3. Differences in bacterial community composition, diversity and structure between healthy and diseased shrimp. (A) Intestinal microbiota composition at the phylum level. (B) Venn diagram analysis depicting the numbers of shared and unique OTUs healthy and diseased shrimp. (C) Non-metric multidimensional scaling (NMDS) and analysis of similarity (ANOSIM) were performed to evaluate the overall differences in bacterial community structure based on Bray-Curtis distance. (D) Intestinal microbiota composition at the family level. (*t*-test followed by Benjamini-Hochberg false discovery rate correction, $^{*}P < 0.05$). (E) Bacterial taxa differentially displayed in healthy and diseased shrimp intestine identified by LEfSe using a LDA score threshold of > 3.5.

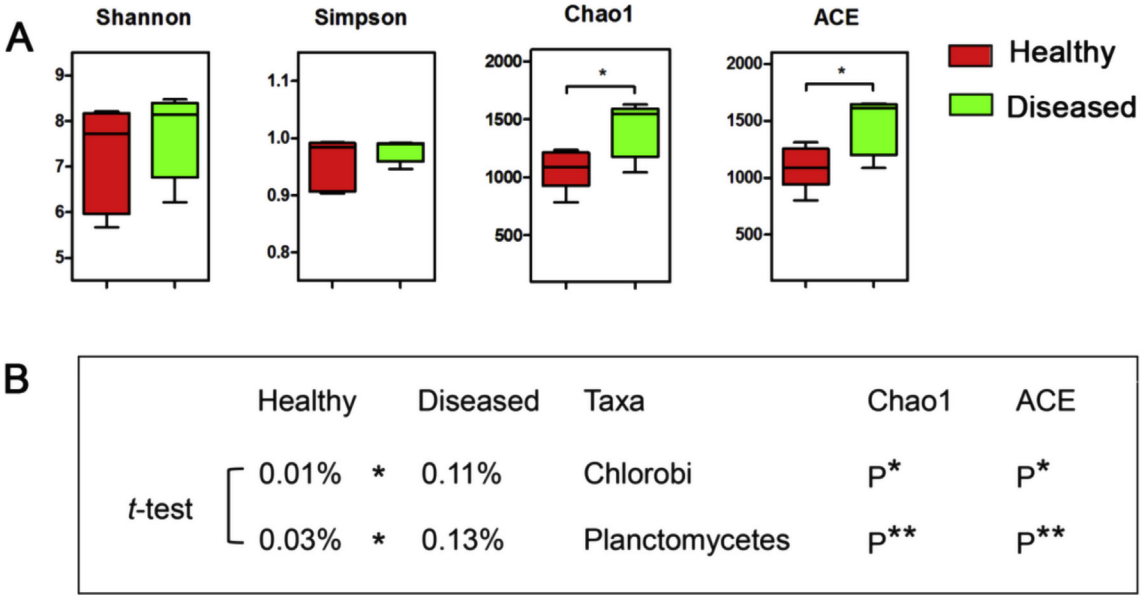

Fig. 4. The α-diversity indices of bacterial community. (A) Box plots depict Shannon, Simpson, ACE and Chao 1 index in intestine microbiota. *$P < 0.05$. (B) Taxa at the phylum level with significant difference between healthy and diseased shrimp (*t*-test, *$P < 0.05$); Spearman's correlation analyses were applied to the correlations between these taxa and richness indices; P, positive correlation; **$P < 0.01$.

(Fig. 3E). The α-diversity of healthy shrimp intestinal microbiota was relatively stable. In contrast, diseased shrimp exhibited a significantly higher Chao1 and ACE index compared with healthy shrimp (Fig. 4A). However, there were no significant differences in Shannon and Simpson index. The relative abundance of phyla *Chlorobi* and *Planctomycetes* were significantly and positively correlated with the Chao1 and ACE index (Fig. 4B). According to the NMDS of Bray-Curtis distance, the healthy and diseased shrimp were clearly separated and formed two distinct clusters owing to the significantly different bacterial communities, which was further confirmed by the analysis of similarity (ANOSIM) test ($R = 0.412$, $P = 0.007$) (Fig. 3C).

3.4. Functional prediction of the intestinal microbiota

Bacterial gene functions were predicted from 16S rRNA sequencing data by using PICRUSt. Comparing the healthy and diseased shrimp, KEGG pathways with significant difference were divided into six categories at KEGG level 1: "Metabolism", "Genetic Information Processing", "Environment Information Processing" "Cellular Processing", "Organismal Systems" (Table 1) and "Human Diseases" (data not shown). Among these pathways, membrane transport and transporters were the firstly and secondly most abundant KEGG pathway. Specifically, most part of pathways (83%) significantly increased in diseased shrimp, whereas pathways involved in other glycan degradation, pyruvate metabolism, membrane transport and transporters significantly decreased.

3.5. Intestine microbiota interspecies interaction

To evaluate the effect of disease outbreak on interspecies interaction of the intestine microbiota, the interspecies interaction network was established. The network was more complex and better connected in healthy shrimp than in diseased shrimp, as evidenced by more links and bigger network size (Fig. 5). This pattern was confirmed by topological properties where the average path of healthy shrimp was higher than that of diseased shrimp (Table 2). The network of healthy shrimp consisted of 43 nodes and 134 edges, which were apparently more than those of the diseased one (38 nodes and 71 edges) (Table 2). Notably, the percentage of positive/negative correlation of bacterial taxa between healthy and diseased shrimp was similar (Table 2).

Table 1
Relative abundance of predicted functions. KEGG level 1 and level 2, as well as level 3 are listed.

KEGG level	KEGG pathway	Healthy (%)	Diseased (%)	p-value
1	Metabolism			
2	Enzyme Families	1.655	1.732	0.006
3	Glycosphingolipid biosynthesis	0.020	0.030	0.023
3	Other glycan degradation	0.088	0.056	0.012
3	Peptidases	1.373	1.452	0.002
3	Primary bile acid biosynthesis	0.011	0.015	0.049
3	Pyruvate metabolism	1.200	1.177	0.034
3	Beta-Lactam resistance	0.016	0.021	0.018
1	**Genetic Information Processing**			
2	Transcription	2.288	2.345	0.039
1	**Environmental Information Processing**			
2	Membrane Transport	12.295	11.661	0.035
2	Signaling Molecules and Interaction	0.153	0.177	0.007
3	CAM ligands	0.001	0.002	0.009
3	ECM-receptor interaction	0.001	0.002	0.005
3	Transporters	6.204	5.779	0.028
1	**Cellular Processes**			
2	Cell Communication	0.001	0.002	0.001
3	Focal adhesion	0.001	0.002	0.003
3	Lysosome	0.038	0.061	0.022
1	**Organismal Systems**			
2	Digestive System	0.030	0.041	0.014
2	Immune System	0.042	0.051	0.012
3	Antigen processing and presentation	0.014	0.018	0.020
3	Carbohydrate digestion and absorption	0.006	0.009	0.025
3	NOD-like receptor signaling pathway	0.017	0.023	0.021
3	Progesterone-mediated oocyte maturation	0.014	0.018	0.019
3	Protein digestion and absorption	0.007	0.014	0.016

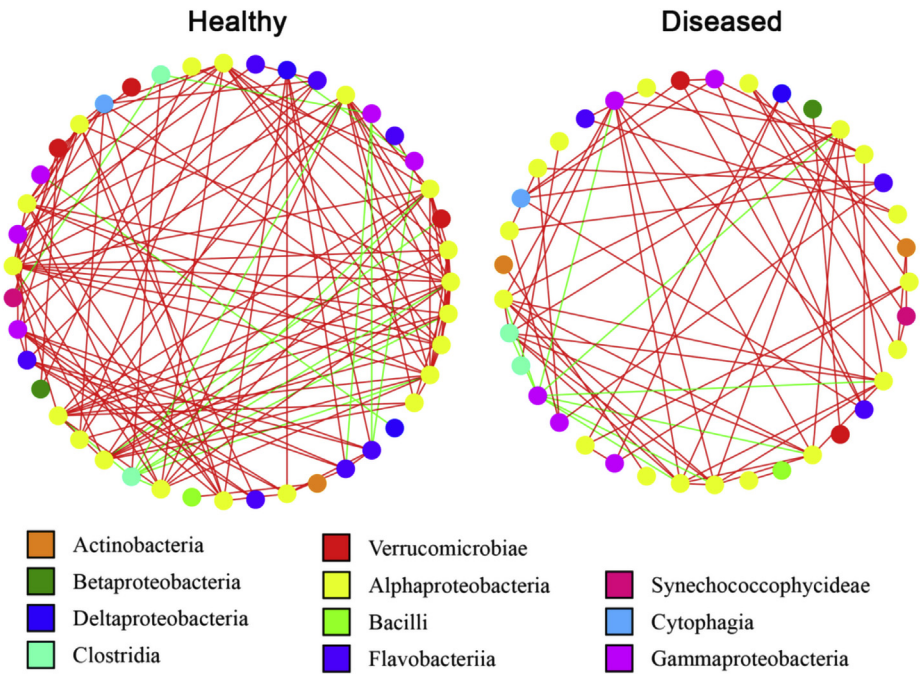

Fig. 5. Interspecies interaction network of intestinal microbiota for healthy and diseased shrimp. Each node represents a bacterial OTU. Node colors indicate OTUs affiliated to different major classes. A blue edge indicates positive interaction, whereas a red edge indicates negative interaction between two individual nodes. (For interpretation of the references to color in this figure legend, the reader is referred to the Web version of this article.)

Table 2
Topological properties of intestinal microbiota co-occurrence network.

	Healthy	Diseased
Node	43	38
Edge	134	71
Average Degree [a]	6.2	3.7
Diameter	18	1
Graph Density	0.15	0.10
Modularity	0.45	0.70
Average Clustering Coefficient	0.5	1.0
Average Path length	3	1
Positive/negative association (%)	88.81/11.19	88.73/11.27

[a] Node connectivity. It is the connection strength between nodes. A higher average degree means a more complex interaction.

4. Discussion

Based on the condition factor and hepatosomatic index, healthy shrimp showed better growth performance than diseased shrimp. Apparent difference in shrimp growth performance can be attributed to several factors such as dietary nutrition, growth stage of the host, and environment conditions [26,27]. However, the effect of these variables could be excluded from this study as these shrimp were from the same batch and managed under the same husbandry conditions. Thus, the possible difference in growth performance could be attributed to health status, particularly to the occurrence of “cotton shrimp-like” disease. Possible explanation for differential growth performance is that the diseased shrimp allocate more energy to cope with pathogen infection and reduce the proportion of energy allocated to growth [28]. This view is supported by the PICRUSt analysis in our study, the result indicated that some functional genes related to energy metabolism, digestive function are activated in diseased shrimp. Furthermore, the gut microbial interspecies interaction contributes to the role in host digestion and feed efficiency [29] as the increase of shrimp intestinal interspecies interaction is positively associated with the enhanced functional potential of the digestive system [30] to facilitate a higher efficiency in nutrient acquisition. In other studies, overgrown shrimp and obese children also show a more complex gut bacterial interspecies interaction than that in normal growth individuals [31,32]. Similarly, in our study the healthy shrimp had more complex intestinal bacterial interspecies interactions than the diseased shrimp, leading to difference in growth performance.

Bacterial pathogens, host microbiota, and the immune system interact with each other to influence the overall functionality in shrimp. Several non-specific immune genes including penaeidin-3a, crustin, ALF, ProPO, Toll and IMD gene, play important roles against pathogen infection in shrimp [33]. In our study, the significant reduction in the expression of those immune genes suggests that the immune system of diseased shrimp has been severely damaged. Host immunity may work synergistically with intestinal commensal bacteria to provide resistance to pathogen colonization [34]. A previous study shows that immunosuppressed patients may have disrupted microbiota that facilitate pathogen colonization in the host [35]. In this regard, we speculate that low immune response will increase susceptibility to pathogens, and thus enhance proliferation of pathogens, such as *Rickettsiaceae* and *Tenacibaculum*. As a result, the immune system of the diseased shrimp can be further damaged by the proliferation of pathogens.

The dominant phylum in the shrimp intestine were *Proteobacteria*, *Tenericutes* and *Bacteroidetes* in this study, though other studies found that *Proteobacteria* is the most abundant phyla in *Litopenaeus vannamei* [36,37]. At the family level, *Rickettsiaceae* was exclusively dominant in the intestine of diseased shrimp. Many species of *Rickettsiaceae* are pathogenic bacteria that might be lethal to shrimp or health deterioration [38]. A previous study has reported that acute phase of the necrotizing hepatopancreatitis was caused by *Rickettsiaceae* [39], and the obvious clinical signs of this disease are a reduction in feeding activity, an empty intestine, flaccid muscle and exoskeleton, and atrophy of hepatopancreas. These are similar to the symptom of the “cotton shrimp-like” disease. Moreover, in other previous study, it was observed that the abundance of *Rickettsiales* significantly increased in diseased shrimp compared with healthy shrimp [40]. Consequently, we speculate that *Rickettsiaceae* was most likely to cause the emergence of “cotton shrimp-like” disease. LEfSe analysis showed that class *Actinobacteria* was a biomarker taxon in the intestine of healthy shrimp with significant higher abundance compared with diseased shrimp. In contrast, the order of *Clostridiales* was a biomarker taxon in the intestine of diseased shrimp with significant higher abundance compared with healthy shrimp. Similarly, this pattern was also detected in the intestinal microbiota of *Plecoglossus altivelis* during *Vibrio anguillarum* infection [2]. LEfSe analysis showed that the genus *Tenacibaculum* was

biomarker in diseased shrimp. Some members of *Tenacibaculum* are known fish pathogens [41], therefore, this pathogens might contribute to cause "cotton shrimp-like" disease. The phylum *Chlorobi* and *Planctomycetes* were significantly and positively correlated with the Chao1 and ACE index, which indicate that those bacterial might contribute to the significant increase of bacterial richness in diseased shrimp.

In diseased shrimp, a large proportion of KEGG pathways including energy metabolism significantly increased. It seems that the up-regulation of these energy production pathways facilitates energy-dependent detoxification as well as other energy-dependent biological processes to help cells to adapt to the changing environment caused by disease infection [42]. Similarly, functional genes related to metabolism are activated during disease infection in shrimp [43]. Membrane transport and transporters were the most abundant KEGG pathways in this study. Since membrane transport and transporters are the largest known protein families and are widely spread in bacteria, it is possible that these pathways are in high abundance in the intestinal microbiota [36]. Bacteria focal adhesion is a virulence factor of bacterial pathogens causing infection [44]. Similarly, the abundance of genes involved in focal adhesion remarkably increased in shrimp with the white feces syndrome [5]. Similarly, in our result the focal adhesion pathways were significantly enriched in the intestine of diseased shrimp. Furthermore, KEGG pathways related to the digestive system significantly increased in diseased shrimp in the present study. As shrimp infected with a disease showed slow growth due to impaired nutrient intake and absorption, an increase of digestive activity may enhance nutrient availability in diseased shrimp. However, PICRUSt is only a means of predicting bacterial function; thus, further research is required to confirm the accuracy of bacterial function information by meta-genomic analysis.

Intestinal microbiota contains a diverse of species interacting with each other and forms a complex ecological network [45,46]. The complexity among intestine microbiota can be compromised in diseased shrimp [4,30]. Our result reveals that the network complexity decreases in diseased shrimp. This result is supported by the view that decreased complexity is prone to invasion by external strains [2]. However, the network complexity increases when a disease occurs [30]. Thus, the relationship between complexity of bacterial interaction network and the emergence of a shrimp disease remains unclear, and future research in this area is needed.

In conclusion, dysbiosis of the composition, diversity, microbial-mediated function and bacterial interaction in intestinal microbiota is closely associated with the "cotton shrimp-like" disease. Exclusively enriched pathogen within family *Rickettsiaceae* and overgrowth of the pathogen within genus *Tenacibaculum* are an indication of low immune response and might result in the occurrence of "cotton shrimp-like" disease. Reduction in complexity of interspecies interaction and disturbance of microbial-mediated function are most likely related to poor growth performance in shrimp with the "cotton shrimp-like" disease infection. These findings significantly improve our understanding on the relationship between dysbiosis of microbiota and the occurrence of "cotton shrimp-like" disease, and provide a guidance for shrimp disease prevention and control through monitoring and regulation on the change of microbial community in the intestine.

Acknowledgments

This study was supported by grants from the Key Research and Development Project of Hainan Province (ZDYF2019068), the National Key Research and Development Program for "Blue Granary" of China (2018YFD0900400), and the initial fund from Hainan University for R & D (KYQD(ZR)1736.

References

[1] J. Libertucci, V.B. Young, The role of the microbiota in infectious diseases, Nat. Microbiol. 4 (2019) 35–45.
[2] L. Nie, et al., Interplay between the gut microbiota and immune responses of ayu (Plecoglossus altivelis) during Vibrio anguillarum infection, Fish Shellfish Immunol. 68 (2017) 479–487.
[3] J. Xiong, et al., Changes in intestinal bacterial communities are closely associated with shrimp disease severity, Appl. Microbiol. Biotechnol. 99 (2015) 6911–6919.
[4] Z. Yao, et al., Disease outbreak accompanies the dispersive structure of shrimp gut bacterial community with a simple core microbiota, Amb. Express 8 (2018) 120.
[5] D. Hou, et al., Intestinal bacterial signatures of white feces syndrome in shrimp, Appl. Microbiol. Biotechnol. 102 (2018) 1–9.
[6] J. Wang, et al., White spot syndrome virus (WSSV) infection impacts intestinal microbiota composition and function in Litopenaeus vannamei, Fish Shellfish Immunol. 84 (2018) 130–137.
[7] W.Y. Chen, et al., Microbiome dynamics in a shrimp grow-out pond with possible outbreak of acute hepatopancreatic necrosis disease, Sci. Rep. 7 (2017) 9395.
[8] F. Cornejo-Granados, et al., Microbiome of Pacific Whiteleg shrimp reveals differential bacterial community composition between Wild, Aquacultured and AHPND/EMS outbreak conditions, Sci. Rep. 7 (2017) 11783.
[9] J. Xiong, W. Dai, C. Li, Advances, challenges, and directions in shrimp disease control: the guidelines from an ecological perspective, Appl. Microbiol. Biotechnol. 100 (2016) 6947–6954.
[10] P. Ramasamy, R. Jayakumar, G.P. Brennan, Muscle degeneration associated with cotton shrimp disease of Penaeus indicus, J. Fish Dis. 23 (2000) 77–81.
[11] S. Yuliya, et al., Morphology and phylogeny of Agmasoma penaei (Microsporidia) from the type host, Litopenaeus setiferus, and the type locality, Louisiana, USA, Int. J. Parasitol. 45 (2015) 1–16.
[12] P.F. Ji, C.L. Yao, Z.Y. Wang, Immune response and gene expression in shrimp (Litopenaeus vannamei) hemocytes and hepatopancreas against some pathogen-associated molecular patterns, Fish Shellfish Immunol. 27 (2009) 563–570.
[13] Y. Sha, et al., Effects of lactic acid bacteria and the corresponding supernatant on the survival, growth performance, immune response and disease resistance of Litopenaeus vannamei, Aquaculture 452 (2016) 28–36.
[14] M. Jin, et al., Dietary yeast hydrolysate and brewer's yeast supplementation could enhance growth performance, innate immunity capacity and ammonia nitrogen stress resistance ability of Pacific white shrimp (Litopenaeus vannamei), Fish Shellfish Immunol. 82 (2018) 121–129.
[15] B.A. Maralit, et al., Differentially expressed genes in hemocytes of Litopenaeus vannamei challenged with Vibrio parahaemolyticus AHPND (VPAHPND) and VPAHPND toxin, Fish Shellfish Immunol. 81 (2018) 284–296.
[16] H.K. Miandare, et al., Dietary Immunogen® modulated digestive enzyme activity and immune gene expression in Litopenaeus vannamei post larvae, Fish Shellfish Immunol. 70 (2017) 621–627.
[17] Y. Duan, et al., Effect of dietary Clostridium butyricum on growth, intestine health status and resistance to ammonia stress in Pacific white shrimp Litopenaeus vannamei, Fish Shellfish Immunol. 65 (2017) 25–33.
[18] J. Gao, et al., Long-term influence of cyanobacterial bloom on the immune system of Litopenaeus vannamei, Fish Shellfish Immunol. 61 (2017) 79–85.
[19] J.G. Caporaso, et al., QIIME allows analysis of high-throughput community sequencing data, Nat. Methods 7 (2010) 335–336.
[20] R.C. Edgar, Search and clustering orders of magnitude faster than BLAST, Bioinformatics 26 (2010) 2460–2461.
[21] T.Z. DeSantis, et al., Greengenes, a chimera-checked 16S rRNA gene database and workbench compatible with ARB, Appl. Environ. Microbiol. 72 (2006) 5069–5072.
[22] Ø. Hammer, D.A. Harper, P.D. Ryan, PAST: paleontological statistics software package for education and data analysis, Palaeontol. Electron. 4 (2001) 1–9.
[23] N. Segata, et al., Metagenomic biomarker discovery and explanation, Genome Biol. 12 (2011) R60.
[24] M.G. Langille, et al., Predictive functional profiling of microbial communities using 16S rRNA marker gene sequences, Nat. Biotechnol. 31 (2013) 814–821.
[25] M. Bastian, S. Heymann, M. Jacomy, Gephi: an open source software for exploring and manipulating networks, Third International AAAI Conference on Weblogs and Social Media, 2009.
[26] W. Dai, et al., The gut eukaryotic microbiota influences the growth performance among cohabitating shrimp, Appl. Microbiol. Biotechnol. 101 (2017) 6447–6457.
[27] T. Forberg, et al., Correlation between microbiota and growth in mangrove killifish (kryptolebias marmoratus) and atlantic cod (Gadus morhua), Sci. Rep. 6 (2016) 21192.
[28] L. Zhou, et al., Environmental concentrations of antibiotics impair zebrafish gut health, Environ. Pollut. 235 (2018) 245–254.
[29] S. Combes, et al., Engineering the rabbit digestive ecosystem to improve digestive health and efficacy, Animal 7 (2013) 1429–1439.
[30] J. Zhu, et al., Contrasting ecological processes and functional compositions between intestinal bacterial community in healthy and diseased shrimp, Microb. Ecol. 72 (2016) 975–985.
[31] J. Xiong, et al., The underlying ecological processes of gut microbiota among cohabitating retarded, overgrown and normal shrimp, Microb. Ecol. 73 (2017) 988–999.
[32] A. Riva, et al., Pediatric obesity is associated with an altered gut microbiota and discordant shifts in F irmicutes populations, Environ. Microbiol. 19 (2017) 95–105.
[33] F. Li, J. Xiang, Recent advances in researches on the innate immunity of shrimp in China, Dev. Comp. Immunol. 39 (2013) 11–26.
[34] C.-Y. Leung, J.S. Weitz, Not by (good) microbes alone: towards immunocommensal therapies, Trends Microbiol. 27 (2019) 294–302.
[35] Y. Taur, E.G. Pamer, The intestinal microbiota and susceptibility to infection in immunocompromised patients, Curr. Opin. Infect. Dis. 26 (2013) 332.
[36] S. Zeng, et al., Composition, diversity and function of intestinal microbiota in

pacific white shrimp (Litopenaeus vannamei) at different culture stages, Peer J. 5 (2017) e3986.
[37] Y. Zheng, et al., Comparison of cultivable bacterial communities associated with Pacific white shrimp (Litopenaeus vannamei) larvae at different health statuses and growth stages, Aquaculture 451 (2016) 163–169.
[38] T. Gollas-Galván, M. Martínez-Porchas, J. Hernandez-Lopez, Rickettsia-like organisms from cultured aquatic organisms, with emphasis on necrotizing hepatopancreatitis bacterium affecting penaeid shrimp: an overview on an emergent concern, Rev. Aquacult. 6 (2014) 256–269.
[39] M. Martínez Porchas, Physiological and immune response of Litopenaeus vannamei undergoing the acute phase of the necrotizing hepatopancreatitis disease and after being treated with oxytetracycline and florfenicol, Lat. Am. J. Aquat. Res. 44 (2017) 535–545.
[40] J. Xiong, J. Zhu, D. Zhang, The application of bacterial indicator phylotypes to predict shrimp health status, Appl. Microbiol. Biotechnol. 98 (2014) 8291–8299.
[41] S. Miyake, et al., Insights into the Microbiota of Asian Seabass (Lates calcarifer) with Tenacibaculosis Symptoms and Description of Sp. Nov, *Tenacibaculum singaporense*. bioRxiv, 2018, p. 472001.
[42] H.-C. Wang, et al., Protein expression profiling of the shrimp cellular response to white spot syndrome virus infection, Dev. Comp. Immunol. 31 (2007) 672–686.
[43] J.P. Apún-Molina, et al., Influence of stocking density and exposure to white spot syndrome virus in biological performance, metabolic, immune, and bioenergetics response of whiteleg shrimp Litopenaeus vannamei, Aquaculture 479 (2017) 528–537.
[44] K.A. Kline, et al., Bacterial adhesins in host-microbe interactions, Cell Host Microbe 5 (2009) 580–592.
[45] K.Z. Coyte, J. Schluter, K.R. Foster, The ecology of the microbiome: networks, competition, and stability, Science 350 (6261) (2015) 663–666.
[46] K. Faust, J. Raes, Microbial interactions: from networks to models, Nat. Rev. Microbiol. 10 (2012) 538–550.